Microchimica Acta (2022) 189: 111
https://doi.org/10.1007/s00604-022-05187-8

ORIGINAL PAPER

Separation and detection of *E. coli* O157:H7 using a SERS-based microfluidic immunosensor

Sara Asgari[1] · Rajiv Dhital[1] · S. Ali Aghvami[2] · Azlin Mustapha[1] · Yi Zhang[3,4] · Mengshi Lin[1]

Received: 18 October 2021 / Accepted: 11 January 2022 / Published online: 19 February 2022

Keywords Food-borne pathogen · Raman spectroscopy · Immunoassay · Food safety · Gold nanoparticles

Abstract

A sensitive SERS-based microfluidic immunosensor was developed to separate and detect *Escherichia coli* O157:H7 in romaine lettuce. SERS nanoprobes, containing gold nanoparticles and specific antibodies against *E. coli* O157:H7, were used to selectively anchor onto the *E. coli* O157:H7 cells and separate them from lettuce samples. Separated cells were then detected within a hydrodynamic flow-focusing microfluidic device using the Raman spectroscope with an excitation laser of 785 nm at ~35 mW. Bacterial concentrations of 100, 10, 1, and 0.5 CFU·mL^{-1} were successfully detected after less than 60 min of enrichment. The limit of detection of *E. coli* O157:H7 in romaine lettuce was found to be 0.5 CFU·mL^{-1}, verifying the sensitivity of our protocol for detection of pathogens in food samples. High linearity ($R^2 > 0.93$) in the calibration curves for *E. coli* O157:H7 was observed after 30 min of enrichment. The method reduced the analysis time for single-cell detection to only 1 h, which is significantly shorter than the days required in conventional methods. In summary, combining the hydrodynamic flow-focusing microfluidic device with SERS nanoprobes provides a reliable, selective, and sensitive approach for the detection of various pathogens in complex food samples.

✉ Mengshi Lin
linme@missouri.edu

[1] Food Science Program, Division of Food, Nutrition & Exercise Sciences, University of Missouri, Columbia, MO 65211, USA

[2] Department of Molecular Metabolism, Harvard University, Boston, MA 02115, USA

[3] Department of Biomedical Engineering, University of Connecticut, Storrs, CT 06269, USA

[4] Polymer Program, Institute of Materials Science, University of Connecticut, Storrs, CT 06269, USA

Introduction

In the USA, the consumption of fresh fruits and vegetables is increasing among consumers. Since these products are mainly consumed raw and are minimally processed, the prevalence of multistate outbreaks of foodborne illnesses associated with raw fruits and vegetables has become an increasing concern recently [1]. Among fresh produce, leafy greens are the most foreseeable implicated vehicles of pathogen hazards [2]. Among bacterial pathogens, Shiga toxin-producing *Escherichia coli* (STEC) are the main foodborne pathogens associated with these outbreaks [3]. Notably, more than half (54%) of the outbreaks were linked to a specific leafy vegetable (i.e., contaminated romaine lettuce), rather than mixed products [4]. The frequently occurring leafy greens-associated outbreaks highlight the importance of early detection of *E. coli* O157:H7 in leafy greens for preventing further contamination over the production and processing chains.

Currently, conventional culture-based isolation and detection methods are used as gold standard methods for the detection of foodborne pathogens. Isolation and detection of *E. coli* O157:H7 in foods involve sample collection, serial dilution, plating, and culturing on selective media, such as sorbitol-MacConkey agar (SMAC) [5]. Despite being simple, inexpensive, and sensitive, these methods are laborious and time-consuming, taking up to 1 week to obtain results [6]. Likewise, if the number of bacteria in the food sample is low, these methods require enrichment of bacterial cells with an extra 8–24 h prior to the detection [7]. Currently, culture-independent methods, such as nucleic acid-based methods and immunoassays have been widely used as alternative methods to overcome the drawbacks of conventional methods due to their higher sensitivity, specificity, and rapidity [8]. Nucleic acid-based methods such as polymerase chain reaction (PCR) involve the detecting specific target genes

or DNA sequences of target pathogens using a thermostable polymerase enzyme [9]. These methods are considered sensitive and rapid methods as low concentrations of foodborne pathogens can be detected within hours. However, these techniques may bring other limitations to the detection procedure, such as high costs, the requirement for trained personnel and sophisticated devices, and several technical issues, especially when used for complex matrices [10]. Immunoassays such as enzyme-linked immunosorbent assay (ELISA) are qualitative-quantitative tests that are based on the interaction of a specific antibody with a target antigen [11]. Accordingly, there are commercial antibody-based kits developed for fast, on-site detection of *E. coli* O157:H7. However, their suitability for monitoring a low initial concentration level of bacteria is still questionable [12].

Surface-enhanced Raman spectroscopy (SERS)-based immunosensors have been recently recognized as a powerful clinical and biochemical diagnosis method. Generally, these methods are operated by (i) SERS tags that include antibodies to anchor onto bacterial cells, (ii) SERS reporter molecules, and (iii) SERS active substrates [13]. The superiority of this technique over conventional immunoassay methods, such as ELISA and fluorescence-based assays, lies in the fact that (i) SERS has a relatively high sensitivity even at very low concentrations of the target analytes [14, 15], (ii) less susceptibility of Raman signals to photobleaching results in lower detection limits [16], (iii) multiplexing is achievable using multiple complementary antibodies and different Raman reporters [17], and (iv) narrow Raman signals facilitate the detection of multiple biomarkers and pathogens [18]. Nonetheless, inconsistent and irreproducible SERS results cause difficulties in quantitative analysis [19]. Therefore, the integration of SERS-based immunoassay into a microfluidic channel provides a homogeneous analysis condition, facilitating accurate quantitative evaluation of the target analytes [19]. Additionally, this platform offers automatic sampling, continuous and multiplex analysis with low sample consumption [20].

Various SERS-based microfluidic immunosensors have been evaluated to detect pathogens in recent years. Each research group developed a specific strategy to lower the limit of detection (LOD). Integration of SERS tags into a microfluidic dielectrophoresis sensor led to a very low LOD of 70 CFU·mL^{-1} [21]. However, inefficient liquid from such sensors usually results in incompetent quantitative detection of bacteria in complex samples [22]. A nano-dielectrophoretic microfluidic sensor coupled with SERS was employed for online enrichment, separation, and detection of *E. coli* O157:H7 in water [23]. Although the method is highly sensitive and all steps were applicable in one step, the technique is too complicated and lacks applicability when bacteria exist in food samples [24]. Off-chip labeling was another technique used to separate and detect *Listeria monocytogenes* in pure culture [25]. This study achieved a very high LOD value of 10^5 CFU·mL^{-1}, which is too high for highly pathogenic bacteria. Therefore, it is necessary to develop an efficient, rapid, and feasible method to detect *E. coli* O157:H7 in complex food samples with high sensitivity and selectivity.

Herein, we developed a feasible and sensitive protocol to separate and detect pathogens in complex food samples. Our study targeted the detection of *E. coli* O157:H7 in romaine lettuce because of the importance of this pathogen in leafy greens, specifically lettuce. Our protocol consists of (1) an enrichment step, (2) off-chip separation and labeling of pathogens by fluorescent immune-nanoprobes in the food sample, and finally (3) on-chip detection of the labeled bacterial cells by a sensitive SERS microchip which is capable of detecting individual cells in a thin layer of fluid flow. Remarkably, our protocol showed excellent separation and detection performance of the very low counts of pathogens in complex food samples. The detection time was much less than that of standard conventional methods. The results of this study are promising for the practical separation and detection of pathogens in food samples. To the best of our knowledge, there is no reported study on separation and detection of *E. coli* O157:H7 using SERS-based microfluidic immunosensors with a LOD value of less than 10^2 CFU·mL^{-1} in the food sample.

Materials and methods

Chemicals and materials

Au nanoparticles (AuNPs) were fabricated by the citrate reduction technique based on a previous method [26]. In brief, AuNPs were fabricated by reducing Au^{3+} ions using a mild reducing and stabilizing agent, trisodium citrate, in an aqueous medium. SERS nanoprobes were prepared according to the modified protocol described by [27]. The detailed chemicals list and SERS-nanoprobes synthesis were provided in the Electronic Supplementary Materials (ESM).

Bacterial cocktail preparation

Three strains of STEC O157:H7 (Table 1) isolated from different sources were selected to prepare a cocktail for

Table 1 *E. coli* O157:H7 strains used in this study

O-serogroup	Strain	Source
E. coli O157:H7	505B	Beef (FRI)
E. coli O157:H7	93-111	Hamburger
E. coli O157:H7	EDL-933	Human (USA)

inoculation into the lettuce samples. First, each strain was separately grown overnight in fresh TSB broth at 37 °C. After incubation, the bacterial pellets were collected by centrifugation at 11200 ×*g* and suspended in sterile peptone water. Bacterial counts for each strain were obtained by performing serially diluting and pour plate counting colonies on TSA. Bacterial colonies for each strain were enumerated after incubation at 37 °C for 24 h. Based on the number of CFU·mL^{-1} counts obtained for each strain, corresponding dilutions and volumes were determined to get a cocktail with a ratio of 1:1:1 for each strain. Finally, the cocktail was serially diluted to obtain spiking inoculums of 0.1, 0.5, 1, 10, and 100 CFU·mL^{-1}.

Sample preparation

Prior to inoculation of the spiking cocktail into the lettuce samples, the purchased samples were evaluated for the presence of STEC O157:H7. More details can be found in ESM. Lettuce samples were prepared by cutting lettuce leaves into pieces of roughly the same size. The prepared lettuce samples (200 g each) were placed in sterile stomacher® bags and spiked with 1 mL of 0.1, 0.5, 1, 10, and 100 CFU·mL^{-1} of *E. coli* O157:H7 cocktail. After inoculation, the samples were left for 15 min to allow bacterial cells to attach to the leaves' surfaces. Then, 450 mL of sterile (1×) mBPW with vancomycin (8 mg·L^{-1}), prewarmed at 42 °C, was added to the samples and the bags were hand-massaged thoroughly for 1 min. *E. coli*-inoculated lettuce samples were incubated at 42 °C for 15, 30, 45, 60, and 120 min for enrichment, and sampling for SERS detection was performed [28, 29]. For sampling, 2 mL of the fluid was collected into the centrifuge tube and stored properly until further steps.

Labeling of the bacterial cells

First, 1 mL of glutaraldehyde solution (2.5%) was injected into 1 mL of the sample, followed by storing the samples at 4 °C for 30 min to allow bacterial cells to be fixed. Afterward, the cells were collected by twice washing and centrifugation at 9300 ×*g* for 15 min. The pellets were then mixed and homogenized with 1 mL of SERS-nanoprobe solution followed by incubation in a shaking incubator at 37 °C at a speed of 100 rpm·min^{-1} for 15, 30, 45, and 60 min. After incubation, free reagents and SERS nanoprobes were withdrawn by twice washing and centrifugation at 9300 ×*g* for 15 min. The resulting labeled pellets were resuspended into 1 mL of sterile PBS and stored at 4 °C for further analysis.

Microfluidic channel fabrication

The microchip layout was designed using AUTOCAD 2021 (Autodesk Inc., Mill Valley, CA, USA) with desired dimensions, and PDMS microchip was fabricated according to the techniques of standard photolithography and soft lithography. Briefly, SU-8 2075 was deposited on cleaned silicon wafers in two sequential steps; (i) first spin-coating by spreading (500 rpm for 10 s at an acceleration rate of 100 rpm·s^{-1}), spinning (1000 rpm for 30 s at an acceleration rate of 300 rpm·s^{-1}) and soft-baking (for 60 min at 100 °C); and (ii) second spin-coating by spreading (500 rpm for 7 s at an acceleration rate of 100 rpm·s^{-1}), spinning (3000 rpm for 30 s at an acceleration rate of 300 rpm·s^{-1}), and soft-baking (for 12 min at 100 °C) to reach to a ~220 µ and ~70 µ thickness of the photoresist on the wafer, respectively. UV exposure and development in SU-8 developer resulted in a channel with a depth of ~300 µ. For easier detachment of PDMS, PMMA2 solution was spin-coated and baked for 5 min at 180 °C on silicon wafer. To develop a PDMS microchip, a degassed PDMS mixture was cast on silicone-photoresist mold and left to polymerize at 70 °C for 1 h. The PDMS channel was finally peeled off from the mold and plasma-bonded to a cleaned glass slide.

Detection

To increase the efficiency of the detection performance, a flow-focusing microfluidic device was used in this study. For this purpose, the sample, labeled bacteria suspended in PBS, was injected from inlet B with the flow rate of 5 µL·min^{-1} and two lateral flows of PBS, as neutral flows, were injected from inlets A and C with flow rates of 10 µL·min^{-1} to surround the central sample flow. Raman signals were collected by focusing the Raman laser with a width of ~100 µm on the central stream and ten signals were continuously collected while the sample was flowing through the microchip.

Data collection was performed using a Raman Spectrometer (Renishaw RM1000 System, Gloucestershire, UK) with a 50× objective and an excitation wavelength of 785 nm at ~35 mW. The system is equipped with a microscope (Leica DMLB, Wetzlar, Germany) and a 388 × 578 pixel CCD array detector. SERS spectra were acquired over the range of 400–2000 cm^{-1} with 10 s integration time.

Characterization of SERS nanoprobes

The SERS nanoprobes were characterized by UV-Vis spectroscopy (Cary Bio 50, Agilent, CA, USA) and transmission electron microscopy (TEM) using high-resolution FEI Tecnai F30 Twin TEM operating at 300 kV at different stages of preparation. SEM images were acquired using a FEI Quanta 600 F SEM (FEI, Hillsboro, OR, USA) operated at 10 kV. Confocal microscopy of the labeled bacterial cells was performed with a Leica SP8 laser scanning confocal microscope equipped with a tunable supercontinuum white light laser

and a 63×/NA1.20 water immersion objective. More details can be found in the ESM.

Data analysis

All experiments were repeated three times and in each run of SERS measurement, ten Raman signals were recorded by the WiRE 3.4 software (Gloucestershire, UK).

Results and discussion

Principal of the separation and detection of *E. coli* O157:H7

Herein, a combination of immunoassay, SERS, and microfluidics was used to selectively separate and detect *E. coli* O157:H7 cells in romaine lettuce. The separation and detection are accomplished by fluorescent immune-nanoprobes that can selectively anchor onto *E. coli* O157:H7 cells and have high SERS activity which enables the detection of pathogenic bacteria, even with low counts, in complicated food matrixes. The nanoprobes consist of three important segments: (i) biotin anti-*E. coli* antibodies as the anchoring moiety to selectively capture *E. coli* O157:H7 cells, (ii) R6G molecules as the SERS reporter and as an indicator of the presence of the target bacteria in the sample, and (iii) AuNPs as the SERS active substrate to intensify the Raman signals from the captured bacterial cells. In our proposed protocol, when the food sample is incubated with SERS nanoprobes, the probes are able to anchor and separate bacterial cells from the food matrix due to the avid interaction of antigen with antibody. In the presence of the target pathogen, the separated bacterial cells are further collected and detected in a highly sensitive SERS microchip. However, detection of a single cell in a food sample faces challenges and is not generally straightforward, so having an enrichment step prior to the separation increases the likelihood of rapid detection of a single cell in food samples. Interestingly, our preliminary findings proved that long enrichment periods were not needed compared with traditional methods. Therefore, our proposed method is promising for fast, feasible, and practical applications in a large-scale context.

Fabrication of SERS nanoprobes

The synthesis of the SERS nanoprobe includes a series of reactions that couples AuNPs with the biotinylated antibodies (Fig. S1). For this study, AuNPs of an average particle diameter of 40 nm were used. Commonly, nanoparticles are chemically bonded with antibodies in one of three ways: (i) chemisorption, (ii) via bifunctional molecules, or (iii) through adapter molecules like avidin or streptavidin [30]. The latter approach was used in this study. Streptavidin is a protein that is known and commonly used in immunoassays owing to the strongest non-covalent bond formed with biotin [31]. Streptavidin-functionalized nanoparticles have been used to attach to biotinylated proteins and antibodies [27].

For fabrication of SERS nanoprobes, first, thioctic acid was bonded with AuNPs with its disulfide group at one end [32]. The mixture of EDC and NHS were employed to further activate the carboxyl groups on the other end of thioctic acid molecules [33], enabling binding of thioctic acid to streptavidin upon the addition of streptavidin to thioctic acid-capped AuNPs. Finally, streptavidin was bonded with biotin moiety on the biotinylated antibody through eight hydrogen bonds and also a van der Waals interaction among non-polar groups [31]. R6G, on the other hand, is directly conjugated with AuNP through a strong electrostatic bond [34].

To verify the successful fabrication of SERS nanoprobes, UV-Vis spectroscopy was performed at three points of synthesis. Fig. 1a illustrates a UV–Vis absorption spectrum of SERS nanoprobes at three different fabrication steps. AuNPs showed the maximum absorption at 531 nm, which is typical for AuNPs with a diameter of about 40 nm [35]. A slight redshift was observed in the spectral absorption upon capping AuNPs with thioctic acid and R6G, indicating the variation of the refractive index of AuNPs as the different functionalization layers occur on their surfaces [36]. The surface plasmon band was again redshifted from 536 to 547 nm upon conjugating the particles with antibodies, proving the successful conjugation of antibodies to the nanoparticles [37]. None of these steps significantly affected the size or morphology of AuNPs as shown in TEM images of AuNPs, AuNP@R6G and AuNP@R6G@SA@Ab (Fig. 1b–d).

Anchoring and separation of *E. coli* O157:H7 cells

Bacterial cells collected in food samples were incubated with SERS nanoprobes for different time periods. Based on our preliminary results, the best incubation condition was found to be 30 min at 37 °C with 100 rpm·min^{-1} shaking. TEM and SEM images were used to monitor the attachment of SERS nanoprobes to *E. coli* O157:H7 cells (Fig. 2a, b). These images clearly prove the successful self-assembly of SERS nanoprobes on the bacterial cells. As it is observed, SERS nanoprobes are attached to different regions around the *E. coli* O157:H7 cell. This is explained by the ability of polyclonal antibodies to attach various epitopes of the same antigenic site on the bacterial cell surface [38]. Confocal fluorescent microscopy image (Fig. 2c) also confirmed that SERS nanoprobes were efficiently anchored onto the *E. coli* O157:H7 cell surface. Positioning SERS nanoprobes on bacterial cells creates "hotspots" between the probes on the bacterial

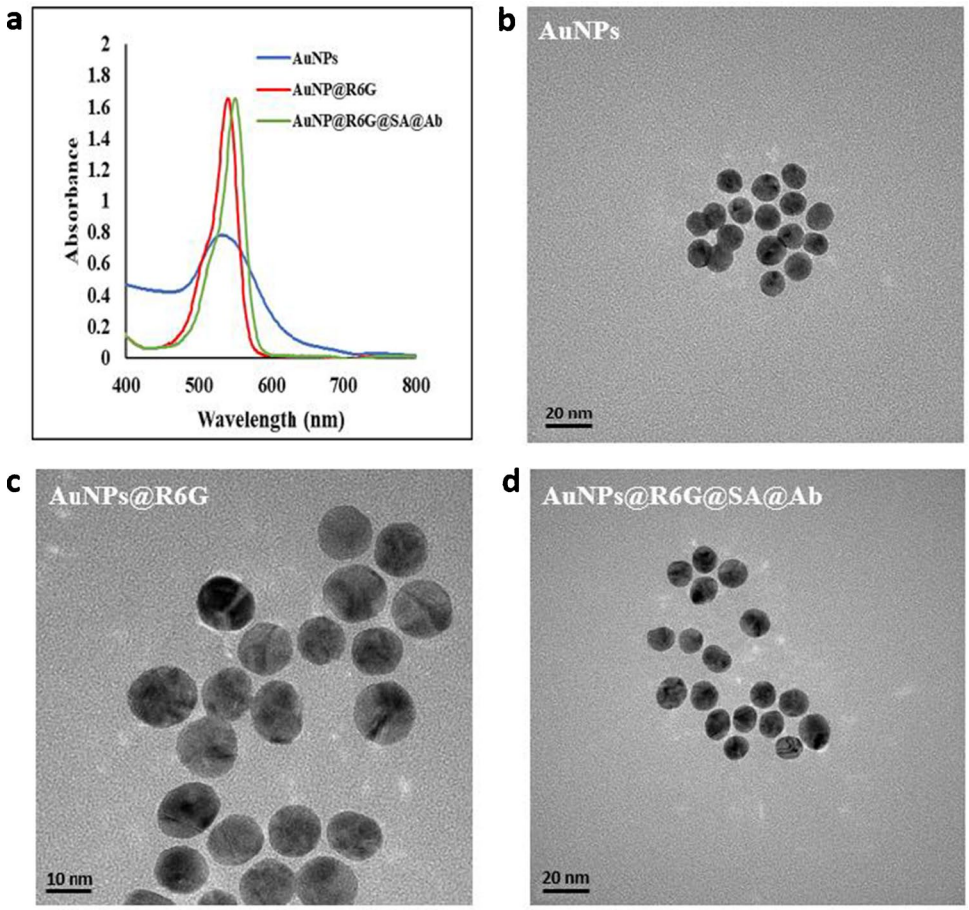

Fig. 1 UV-Vis spectra (**a**) and TEM images (**b**–**d**) of SERS nanoprobes at three different steps of preparation.

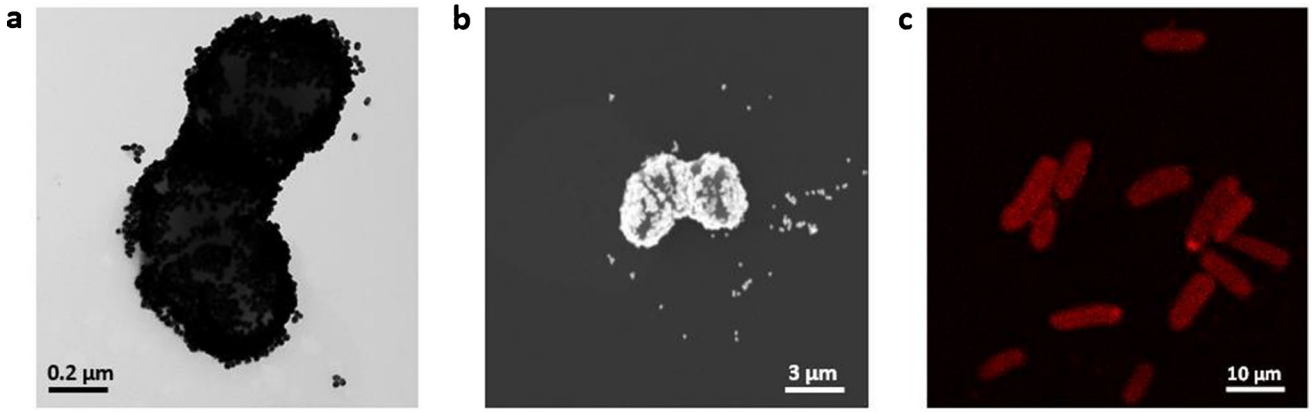

Fig. 2 TEM (**a**), SEM (**b**), and confocal fluorescent microscopy (**c**) images of labeled *E. coli* O157:H7 cells by SERS nanoprobes.

cell surface and between the labeled bacteria, amplifying the Raman signals from separated target bacteria [25, 39]. This results in sharper

Raman signals with higher intensities, leading to a more efficient SERS detection performance.

Fabrication of hydrodynamic flow focusing SERS microchip

In this study, a hydrodynamic flow-focusing microfluidic channel with T-junction was designed for in-flow detection

of incubated *E. coli* O157:H7 cells. The AutoCAD design and fabricated microchip are shown in Fig. S2a and b. The optimized channel was fabricated with a width and depth of 300 µm and a length of 3.5 cm. The microchip is devised and optimized in a hydrodynamic flow-focusing design, offering two advantages for more sensitive detection. The first benefit is that, in such a structure, the central fluid (separated and labeled bacterial cells) flows in a thin layer where a single cell, if present, is detectable [40]. Second, the chance that labeled cells are exposed to the Raman laser increases since bacterial cells are concentrated in the central stream where the Raman laser is focused at [25]. Fig. S2c shows the successful flow-focusing approach obtained in our SERS microchip. The width of the central flow was measured to be about 15 µm.

Detection of *E. coli* O157:H7 cells by SERS-based microfluidic immunosensor

Typical Raman spectra of R6G and AuNP@R6G@SA@Ab SERS nanoprobes are shown in Fig. S3. As seen, the peaks in the SERS-nanoprobe signals represent main Raman peaks of R6G although a small shift is observed due to the presence of other components in the SERS-nanoprobe solution. The main peaks of R6G include 611 (C–C–C ring in-plane bending), 773 (C–H out-of-plane bending), 1197 (C–H out-of-plane bending), 1308 (aromatic C–C stretching), 1358 (aromatic C–C stretching), 1510 (aromatic C–C stretching), 1612 (aromatic C–C stretching), and 1650 cm^{-1} (aromatic C–C stretching) [41]. Among them, the peak at 1510 cm^{-1} is considered the characteristic peak of R6G which is equivalent to 1509 cm^{-1} in SERS-nanoprobe Raman peak. According to plating and immunoassay kits, the original romaine lettuce samples used in this study were not contaminated by *E. coli* O157:H7 prior to the experiments. Fig. 3a–e display SERS signals collected from the detection of *E. coli* O157:H7 at different spiking levels, ranging from 0.1 to 10^2 $CFU{\cdot}mL^{-1}$, and after various incubation times. The signals are in fact the fingerprint Raman signals of R6G, which have been enhanced by AuNPs present in the SERS nanoprobes and indirectly represent *E. coli* O157:H7 in the sample. The images show that the obtained signals were clear and sharp. The changes of SERS signals were consistent with the changes of bacterial counts in lettuce samples, i.e., the SERS intensity concomitantly increased with the increase of *E. coli* O157:H7 concentration. In this way, the intensity of the band 1509 cm^{-1} is the highest for samples spiked by 100 $CFU{\cdot}mL^{-1}$, and then it decreases as the spiking level decreases and reaches zero when bacterial concentration is very low. Likewise, increasing the incubation time improved the sharpness of the peaks and intensity of the signals that were collected from the samples with the same spiking levels.

Table 2 summarizes the findings of this study and presents a better outlook of the capability of SERS-based microfluidic immunosensor to detect *E. coli* O157:H7 cells in lettuce. Accordingly, our protocol was able to detect *E. coli* O157:H7 cells at 100 $CFU{\cdot}mL^{-1}$ after 15 min enrichment. After only 30 min of enrichment, the protocol clearly detected the bacterial cells at the spiking level of 10 and 1 $CFU{\cdot}mL^{-1}$. The results were the same after 45 min of enrichment although longer enrichment time resulted in stronger and clearer signals for all 10^2, 10, and 1 $CFU{\cdot}mL^{-1}$ counts. Further enrichment for 2 h provided even better results. The very low amount of 0.1 $CFU{\cdot}mL^{-1}$ of bacterial cells was not detectable by our protocol, which is considerably lower than the infectious dose of less than 10^2 $CFU{\cdot}mL^{-1}$ for *E. coli* O157:H7 [42].

It is worth noting that, in this method, the total analysis time for detection of a single bacterium in a food sample is only 1 h considering the enrichment time that is significantly less than what is needed (days) in conventional methods. Interestingly, our protocol improved the results compared with the previously reported method [27] owing to the combination of enrichment, off-chip separation, and in-flow detection in a highly efficient SERS microchip. Furthermore, the lowest concentration at which fingerprint-like SERS signals were obtained was 0.5 $CFU{\cdot}mL^{-1}$. Therefore, our method achieved a very low LOD value of 0.5 $CFU{\cdot}mL^{-1}$ after only 60 min of enrichment which is an excellent proof of sensitivity and rapidity of our proposed method.

Intensity-concentration calibration curves for *E. coli* O157:H7 are plotted in Fig. S4, showing obtained SERS intensity at 1509 cm^{-1} versus logarithmic (spiked) concentration of *E. coli* O157:H7 in lettuce after various enrichment times. Increasing the enrichment time after 15 min increased the linearity of the relationship between bacterial concentration and obtained signal (from R^2 of 0.72 to R^2 values of > 0.93), indicating more reliability of the results in enrichment times higher than 15 min.

Figure S5 shows the Raman spectra obtained from PDMS, non-labeled *E. coli* O157:H7 cells, and the mixture of *E. coli* O157:H7 cells and AuNPs. The mixture of bacterial cells and AuNPs resulted in the enhanced signals of bacteria and did not include any other peaks. The peaks of PDMS and *E. coli* O157:H7 cells are not present in the signals obtained from labeled bacterial cells, which means that the signals received from the reporter are dominant and mask any other interfering noises or signals from PDMS, bacteria, and the food matrix.

The reproducibility of our technique was investigated by tracking the variations of SERS signals at the characteristic peak, 1509 cm^{-1}, obtained from samples inoculated with 100 $CFU{\cdot}mL^{-1}$ *E. coli* O157:H7 after 30 and 60 min of incubation at three repetitions (Fig. S6). The obtained signals were almost consistent, proving the reproductivity of

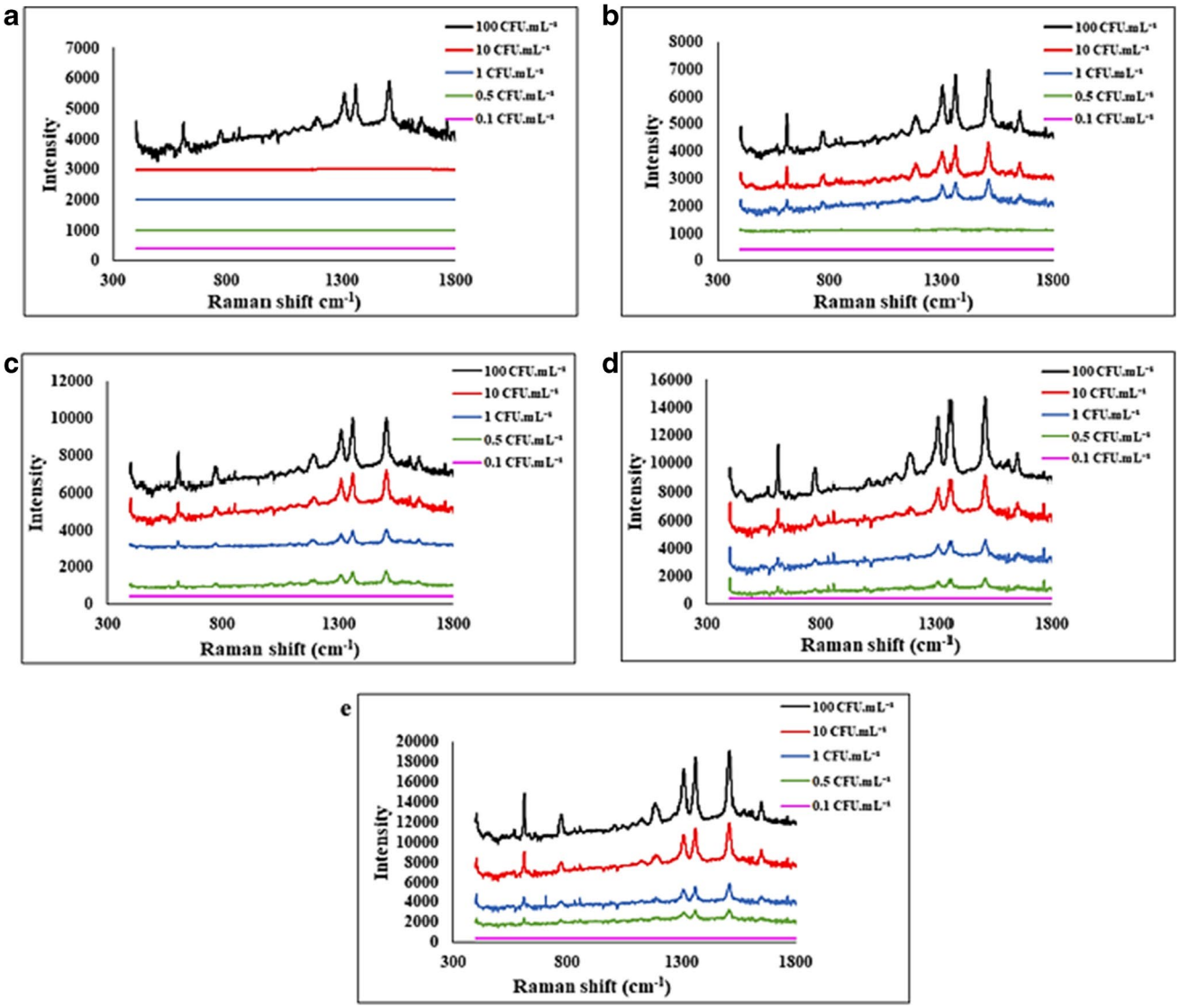

Fig. 3 SERS signals obtained from lettuce samples spiked with *E. coli* O157:H7 at different spiking levels of 0.1, 0.5, 1, 10, and 10^2 CFU·mL^{-1} after 15 min (**a**), 30 min (**b**), 45 min (**c**), 60 min (**d**), and 120 min (**e**) of enrichment.

Table 2 Capability of SERS-based microfluidic immunosensor to detect *E. coli* O157:H7 cells in lettuce

Spiked level (CFU·mL^{-1})	Enrichment time (min)				
	15	30	45	60	120
100	+	+	+	+	+
10	_	+	+	+	+
1	_	+	+	+	+
0.5	_	_	_	+	+
0.1	_	_	_	_	_

our technique for detection of *E. coli* O157:H7 in lettuce. Slight variations observed in the SERS intensities were expectable as the behavior of optical measurement systems. Depending on the sample, however, low-cost thermoplastic microchips offer the possibility for disposable sensors. The stability assessment of the SERS nanoprobes showed that the SERS nanotags were stable for 10 days (at 4 °C in the dark), showing their highest performance to attach to the target bacterial cells.

Table 3 summarizes the findings obtained from recent literature on the use of optical methods for the detection and determination of *E. coli*. Combined immunomagnetic separation and SERS detection methods are usually simpler; however, the uncontrolled analysis conditions may result in high background noises and less sensitivity. Fluorescent sensing is considered a very sensitive detection method, but the degradation of fluorescence may interfere with the accuracy of the results. Methods based on nano-dielectrophoretic

Table 3 An overview on recently reported nanomaterial-based optical methods for the determination of *E. coli*

Principal	Nanomaterial	LOD	Reference
Immunomagnetic separation + SERS	Magnetic nanoparticles + AuNPs	10 CFU·mL^{-1}	[1]
Immunomagnetic separation + SERS	Magnetic gold nanorod	35 CFU·mL^{-1}	[2]
Immunoseparation + Two-Photon Rayleigh Scattering	Gold nanorod	50 CFU·mL^{-1}	[3]
Fabry-Pérot interference	PSi-based Fabry-Pérot thin films	10^3 cells·mL^{-1}	[4]
Fluorescent sensing	Magnetic carbon dots	3.5×10^2 CFU·mL^{-1}	[5]
Optofluidic + fluorescent sensing	Aptamer-conjugated fluorescent nanoparticles	10^2 CFU·S^{-1}	[6]
SERS-based sandwich immunoassay	AuNPs	10 CFU·mL^{-1}	[7]
SERS + nano-dielectrophoretic microfluidic device	Gold nanorods	10 CFU·mL^{-1}	[8]
Immunoseparation + SERS	Au@Ag core-shell nanorod	10^2 CFU·mL^{-1}	[9]
SERS-based microfluidic immunosensor	AuNPs	0.5 CFU·mL^{-1}	This study

microfluidic devices are usually complex and sometimes expensive to handle. The drawbacks associated with SERS-based sandwich immunoassay are the high possibility of cross-reactivity and inconsistent results of SERS measurements in an uncontrolled analysis condition. However, our method is not prone to degradation and is performed in a highly controlled hydrodynamic flow-focusing microfluidic device that was able to achieve a very low LOD value compared to the other methods, proving the high sensitivity of our method against *E. coli* in lettuce and the potentiality of this protocol for detection of pathogens in complex food samples. Although the necessity of the enrichment time in our protocol may increase the total analysis time compared with some of the optical methods, it leads to very high sensitivity for detecting the target pathogen. Regarding the analysis costs, a very low number of antibodies are needed to conduct several analyses that neutralize the high costs of antibodies. Therefore, the cost per analysis is not considered high. This method consists of a series of simple chemical reactions, which can be done by a technician, and the detection step may be automatized for subsequent analyses, which makes this protocol easy to perform.

Selectivity of SERS-based microfluidic immunosensor for *E. coli* O157:H7

Two sets of experiments were used to investigate the selectivity of our method for *E. coli* O157:H7. For the first control experiment, the control samples were inoculated with *Salmonella enteritis* (100 CFU·mL^{-1}), and the incubation, separation, and detection steps were followed as explained earlier under the same conditions by using the SERS nanoprobes specific for *E. coli* O157:H7. Fig. S7a shows that no signals were observed after 30 and 60 min of incubation times, and there were only noises observed in the obtained spectra, proving that SERS nanoprobes containing anti-*E. coli* antibodies did not interact with cells other than *E. coli* O157:H7, and therefore, our method is selective for a specific target. For the second control test, the selectivity of our method was evaluated in the presence of other common pathogens. Lettuce samples were spiked by 1 mL *E. coli* O157:H7 (100 CFU·mL^{-1}), 1 mL *S. Enteritis* (100 CFU·mL^{-1}), and 1 mL *S. Typhimurium* DT104 (100 CFU·mL^{-1}), and the separation and detection were conducted only by SERS nanoprobes specific for *E. coli* O157:H7. The findings were consistent with the results obtained from lettuce samples inoculated by only *E. coli* O157:H7 after 30 and 60 min of incubation (Fig. S7b). No interfering noises were observed since the strong signals from labeled *E. coli* O157:H7 cells masked the weak noise signals from interfering bacterial cells or particulates. Thus, our method is selective for the separation and detection of the target pathogen even in the presence of the interfering species as the real world. It is worth noting that the used SERS nanoprobes are selective for *E. coli* O157:H7 in the presence of other pathogens but do not act selectively for *E. coli* O157:H7 in the presence of *E. coli* K12 strains.

Conclusions

This study developed a novel protocol to selectively separate and sensitively detect *E. coli* O157:H7 in romaine lettuce. This technique combines three steps, an enrichment step, a selective separation with specific SERS nanoprobes, and a sensitive SERS microchip, resulting in a sensitive single-cell detection in food samples. Selective separation is accomplished by SERS nanoprobes containing specific antibodies against the target pathogen. The hydrodynamic flow-focusing SERS microchip designed in this study not only facilitated a sensitive detection of the target bacteria, but also offered the controllability of the analysis conditions, automation, and better repeatability. Furthermore, a short enrichment time of 60 min resulted in the detection of

0.5 CFU·mL^{-1} of bacterial concentration in romaine lettuce, which is much lower than *E. coli* O157:H7 infectious dose. Therefore, our findings prove the reliability and feasibility of the proposed SERS-based microfluidic immunosensor for the sensitive separation and detection of foodborne pathogens in food samples. The generic approach of this study may apply to other food-borne pathogens and other food types. This work can be improved further by using monoclonal antibodies to promote the selectivity of the SERS nanoprobes. Future research will be oriented towards the development of more selective probes. Multiplex detection of pathogens from a single food sample is also possible using multiple SERS nanoprobes, each targeting a specific pathogen.

Supplementary Information The online version contains supplementary material available at https://doi.org/10.1007/s00604-022-05187-8.

Funding This research was financially supported by USDA National Institute of Food and Agriculture (2018-67017-27880, 2019-67021-29859), the National Science Foundation (CBET-2103025), and the Robert T. Marshall Scholarship.

Declarations

Conflict of interest The authors declare no competing interests.

References

1. Yu H, Neal JA, Sirsat SA (2018) Consumers' food safety risk perceptions and willingness to pay for fresh-cut produce with lower risk of foodborne illness. Food Control 86:83–89. https://doi.org/10.1016/J.FOODCONT.2017.11.014
2. FDA (1998) Guidance for industry: guide to minimize microbial food safety hazards for fresh fruits and vegetables | FDA. https://www.fda.gov/regulatory-information/search-fda-guidance-documents/guidance-industry-guide-minimize-microbial-food-safety-hazards-fresh-fruits-and-vegetables. Accessed 19 May 2021
3. CDC (2021) Lettuce, other leafy greens, and food safety | Food Safety | CDC. https://www.cdc.gov/foodsafety/communication/leafy-greens.html. Accessed 27 Aug 2021
4. Marshall KE, Hexemer A, Seelman SL et al (2020) Lessons learned from a decade of investigations of Shiga toxin-producing *Escherichia coli* outbreaks linked to leafy greens, United States and Canada. Emerg Infect Dis 26:2319–2328. https://doi.org/10.3201/eid2610.191418
5. March S, Ratnam S (1986) Sorbitol-MacConkey medium for detection of *Escherichia coli* O157:H7 associated with hemorrhagic colitis. J Clin Microbiol 23:869–872. https://doi.org/10.1128/JCM.23.5.869-872.1986
6. Zhao X, Lin C-W, Wang J, Oh DH (2014) Advances in rapid detection methods for foodborne pathogens. J Microbiol Biotechnol 24:297–312. https://doi.org/10.4014/JMB.1310.10013
7. Sharma H, Mutharasan R (2013) Review of biosensors for foodborne pathogens and toxins. Sensors Actuators B Chem 183:535–549. https://doi.org/10.1016/J.SNB.2013.03.137
8. Saravanan A, Kumar PS, Hemavathy R V., et al (2020) Methods of detection of food-borne pathogens: a review. Environ Chem Lett 2020 191 19:189–207. https://doi.org/10.1007/S10311-020-01072-Z
9. Deisingh AK, Thompson M (2004) Strategies for the detection of *Escherichia coli* O157:H7 in foods. J Appl Microbiol 96:419–429. https://doi.org/10.1111/J.1365-2672.2003.02170.X
10. López-Campos G, Martínez-Suárez J V., Aguado-Urda M, López-Alonso V (2012) Detection, identification, and analysis of foodborne pathogens. 13–32. https://doi.org/10.1007/978-1-4614-3250-0_2
11. Seiichi S, Putalun W, Sornkanok V et al (2018) Enzyme-linked immunosorbent assay for the quantitative/qualitative analysis of plant secondary metabolites. J Nat Med 72:32–42. https://doi.org/10.1007/S11418-017-1144-Z
12. D'Lima CB, Suslow TV (2009) Comparative evaluation of practical functionality of rapid test format kits for detection of *Escherichia coli* O157:H7 on lettuce and leafy greens. J Food Prot 72:2461–2470. https://doi.org/10.4315/0362-028X-72.12.2461
13. Han XX, Cai LJ, Guo J et al (2008) Fluorescein isothiocyanate linked immunoabsorbent assay based on surface-enhanced resonance Raman scattering. Anal Chem 80:3020–3024. https://doi.org/10.1021/AC702497T
14. Asgari S, Sun L, Lin J et al (2020) Nanofibrillar cellulose/Au@Ag nanoparticle nanocomposite as a SERS substrate for detection of paraquat and thiram in lettuce. Microchim Acta 187:1–11. https://doi.org/10.1007/s00604-020-04358-9
15. Asgari S, Wu G, Aghvami SA et al (2021) Optimisation using the finite element method of a filter-based microfluidic SERS sensor for detection of multiple pesticides in strawberry. Food Addit Contam - Part A Chem Anal Control Expo Risk Assess 38:646–658. https://doi.org/10.1080/19440049.2021.1881624
16. Jun BH, Kim JH, Park H et al (2007) Surface-enhanced Raman spectroscopic-encoded beads for multiplex immunoassay. J Comb Chem 9:237–244. https://doi.org/10.1021/cc0600831
17. Kamińska A, Witkowska E, Winkler K et al (2015) Detection of hepatitis B virus antigen from human blood: SERS immunoassay in a microfluidic system. Biosens Bioelectron 66:461–467. https://doi.org/10.1016/j.bios.2014.10.082
18. Lee S, Chon H, Yoon SY et al (2012) Fabrication of SERS-fluorescence dual modal nanoprobes and application to multiplex cancer cell imaging. Nanoscale 4:124–129. https://doi.org/10.1039/c1nr11243k
19. Gao R, Cheng Z, deMello JA, Choo J (2016) Wash-free magnetic immunoassay of the PSA cancer marker using SERS and droplet microfluidics. Lab Chip 16:1022–1029. https://doi.org/10.1039/C5LC01249J
20. Bridle H, Miller B, Desmulliez MPY (2014) Application of microfluidics in waterborne pathogen monitoring: a review. Water Res 55:256–271. https://doi.org/10.1016/J.WATRES.2014.01.061
21. Lin H-Y, Huang C-H, Hsieh W-H et al (2014) On-line SERS detection of single bacterium using novel SERS nanoprobes and a microfluidic dielectrophoresis device. Small 10:4700–4710. https://doi.org/10.1002/SMLL.201401526
22. Chen Y-J, Chen Y-Y, Wang K-H et al (2020) Integration of a thermoelectric heating unit with ionic wind-induced droplet centrifugation chip to develop miniaturized concentration device for rapid determination of salmonella on food samples using antibody-functionalized SERS tags. Sensors (Basel) 20:1–14. https://doi.org/10.3390/S20247177
23. Wang C, Madiyar F, Yu C, Li J (2017) Detection of extremely low concentration waterborne pathogen using a multiplexing self-referencing SERS microfluidic biosensor. J Biol Eng 2017 111 11:1–11. https://doi.org/10.1186/S13036-017-0051-X
24. Weng X, Zhang C, Jiang H (2021) Advances in microfluidic nanobiosensors for the detection of foodborne pathogens. LWT 151:112172. https://doi.org/10.1016/J.LWT.2021.112172

25. Rodríguez-Lorenzo L, Garrido-Maestu A, Bhunia AK et al (2019) Gold nanostars for the detection of foodborne pathogens via surface-enhanced Raman scattering combined with microfluidics. ACS Appl Nano Mater 2:6081–6086. https://doi.org/10.1021/ACSANM.9B01223
26. Xiong Z, Lin M, Lin H, Huang M (2018) Facile synthesis of cellulose nanofiber nanocomposite as a SERS substrate for detection of thiram in juice. Carbohydr Polym 189:79–86
27. Bi L, Wang X, Cao X et al (2020) SERS-active Au@Ag core-shell nanorod (Au@AgNR) tags for ultrasensitive bacteria detection and antibiotic-susceptibility testing. Talanta 220:121397. https://doi.org/10.1016/J.TALANTA.2020.121397
28. Singh P, Mustapha A (2015) Multiplex real-time PCR assays for detection of eight Shiga toxin-producing *Escherichia coli* in food samples by melting curve analysis. Int J Food Microbiol 215:101–108. https://doi.org/10.1016/J.IJFOODMICRO.2015.08.022
29. FDA (2019) Guidelines for the validation of microbiological methods for the FDA foods program, 3rd editio
30. Ijeh MO (2011) Covalent gold nanoparticle-antibody conjugates for sensivity improvement in LFIA. Doctoral dissertation, Staats- und Universitätsbibliothek Hamburg Carl von Ossietzky
31. Hyre DE, Le Trong I, Merritt EA et al (2006) Cooperative hydrogen bond interactions in the streptavidin–biotin system. Protein Sci 15:459. https://doi.org/10.1110/PS.051970306
32. Ghann W, Harris T, Kabir D, et al (2019) Lipoic acid decorated gold nanoparticles and their application in the detection of lead ions. J Nanomed Nanotechnol 10:. https://doi.org/10.35248/2157-7439.19.10.539
33. Wang J, Wu X, Wang C et al (2016) Facile synthesis of Au-coated magnetic nanoparticles and their application in bacteria detection via a SERS method. ACS Appl Mater Interfaces 8:19958–19967. https://doi.org/10.1021/ACSAMI.6B07528
34. Akanny E, Bonhommé A, Commun C, et al (2019) Development of uncoated near-spherical gold nanoparticles for the label-free quantification of *Lactobacillus rhamnosus* GG by surface-enhanced Raman spectroscopy. Anal Bioanal Chem 2019 41121 411:5563–5576. https://doi.org/10.1007/S00216-019-01938-4
35. Thacker V V., Herrmann LO, Sigle DO, et al (2014) DNA origami based assembly of gold nanoparticle dimers for surface-enhanced Raman scattering. Nat Commun 2014 51 5:1–7. https://doi.org/10.1038/ncomms4448
36. Ferhan AR, Jackman JA, Sut TN, Cho N-J (2018) Quantitative comparison of protein adsorption and conformational changes on dielectric-coated nanoplasmonic sensing arrays. Sensors 2018, Vol 18, Page 1283 18:1283. https://doi.org/10.3390/S18041283
37. Kamińska A, Sprynskyy M, Winkler K, Szymborski T (2017) Ultrasensitive SERS immunoassay based on diatom biosilica for detection of interleukins in blood plasma. Anal Bioanal Chem 2017 40927 409:6337–6347. https://doi.org/10.1007/S00216-017-0566-5
38. Cho IH, Bhandari P, Patel P, Irudayaraj J (2015) Membrane filter-assisted surface enhanced Raman spectroscopy for the rapid detection of *E. coli* O157:H7 in ground beef. Biosens Bioelectron 64:171–176. https://doi.org/10.1016/J.BIOS.2014.08.063
39. Bai X, Shen A, Hu J (2020) A sensitive SERS-based sandwich immunoassay platform for simultaneous multiple detection of foodborne pathogens without interference. Anal Methods 12:4885–4891. https://doi.org/10.1039/D0AY01541E
40. Pallaoro A, Hoonejani MR, Braun GB et al (2015) Rapid identification by surface-enhanced raman spectroscopy of cancer cells at low concentrations flowing in a microfluidic channel. ACS Nano 9:4328–4336. https://doi.org/10.1021/acsnano.5b00750
41. Vosgröne T, Meixner AJ (2005) Surface- and resonance-enhanced micro-Raman spectroscopy of xanthene dyes: from the ensemble to single molecules. ChemPhysChem 6:154–163. https://doi.org/10.1002/CPHC.200400395
42. Doyle MP (2013) Food safety: bacterial contamination. Encycl Hum Nutr 2–4:322–330. https://doi.org/10.1016/B978-0-12-375083-9.00124-0